DOE/PC/91285-3

Two Dimensional NMR and NMR Relaxation Studies of Coal Structure

DOE/PC/91285--3

DE92 040500

PROGRESS REPORT

including

the period April 1, 1992 to June 30, 1992

Kurt W. Zilm

Department of Chemistry

Yale University

New Haven, CT 06511

Prepared for the Department of Energy

Agreement No. DE-FG22-91PC91285

DISCLAIMER

This report was prepared as an account of work sponsored by an agency of the United States Government. Neither the United States Government nor any agency thereof, nor any of their employees, makes any warranty, express or implied, or assumes any legal liability or responsibility for the accuracy, completeness, or usefulness of any information, apparatus, product, or process disclosed, or represents that its use would not infringe privately owned rights. Reference herein to any specific commercial product, process, or service by trade name, trademark, manufacturer, or otherwise does not necessarily constitute or imply its endorsement, recommendation, or favoring by the United States Government or any agency thereof. The views and opinions of authors expressed herein do not necessarily state or reflect those of the United States Government or any agency thereof.

MASTER

SEP 0 8 1992

JUL 14 1992

NOTICE

This report was prepared as an account of work sponsored by the United States Government. Neither the United States nor the Department of Energy, nor any of their employees, nor any of their contractors, subcontractors, or their employees, make any warranty, express or implied, or assumes any legal liability or responsibility for the accuracy, completeness, or usefulness of any information, apparatus, product or process disclosed or represents that its use would not infringe on privately-owned rights.

US/DOE Patent Clearance is not required prior to publication of this document.

ABSTRACT

This report covers the progress made on the title project for the project period. Four major areas of inquiry are being pursued. Advanced solid state NMR methods are being developed to assay the distribution of the various important functional groups that determine the reactivity of coals. Special attention is being paid to methods that are compatible with the very high magic angle sample spinning rates needed for operation at the high magnetic field strengths available today. Polarization inversion methods utilizing the difference in heat capacities of small groups of spins are particularly promising. Methods combining proton-proton spin diffusion with ^{13}C CPMAS readout are being developed to determine the connectivity of functional groups in coals in a high sensitivity relay type of experiment. Additional work is aimed at delineating the role of methyl group rotation in the proton NMR relaxation behavior of coals.

Introduction

Quantitative differentiation of the various functional groups in coals by ^{13}C CPMAS NMR methods has provided a great deal of structural information which is not available from other spectral techniques. Methods such as dipolar dephasing or magic angle spinning separated local field spectroscopy differentiate carbon centers based on the number of dipolar couplings a given ^{13}C nucleus has to directly attached ^{1}H nuclei. Such methods work as long as one can assume that all ^{13}C-^{1}H dipolar couplings are basically of the same strength. When significant molecular mobility is present or a wide variation in dipolar couplings is encountered these techniques then fail. In this report we present the development of a new method using polarization inversion which can differentiate between CH_3, CH_2, CH and C centers. The new technique is different in that it does not rely heavily upon the strength of the dipolar couplings but instead primarily upon the number of protons attached to a given carbon center. The method is relatively user friendly and can be implemented on a wide range of commercial hardware. In the attached preprint we describe the underlying principles of the method and demonstrate its utility with a number of model compounds. Work is in progress to assess the applicability of the technique to coals.

Complete Spectral Editing in CP /MASS NMR

Xiaoling Wu, and Kurt W. Zilm, Department of Chemistry,
Yale University, New Haven, Connecticut 06511

ABSTRACT

A simple scheme for complete spectral editing of ^{13}C CP/MASS spectra of solids is proposed which can distinguish CH, CH_2, CH_3 and C carbon resonances. It makes use of the fact that the ratios of the heat capacities of the carbon and proton spins for these groups are quite different. The method consists of a polarization inversion (PI) period inserted into the standard CP/MASS experiment. As the PI time increases, the ^{13}C signal intensity decreases at first, passes through zero, and finally becomes negative. Signals for rigid CH and CH_2 groups change rapidly during the first tens of microseconds during PI and then vary at a much slower rate. Typical PI times needed to null the ^{13}C signals are 25, 40, 110 and 350 microseconds for CH_2, CH, CH_3 and nonprotonated C signals, respectively. At the turning point of the fast and the slow PI stages, the CH_2 signals become negative and have a relative intensity of one-third with respect to that before polarization inversion, while the residual CH signal is nearly zero. Consequently, different kinds of carbon signals can be distinguished with ease. Since the relative intensity of CH_n signals at the turning point is not particularly sensitive to molecular motions, this approach is more reliable than methods which rely upon the strength of ^{13}C-^{1}H dipolar couplings.

INTRODUCTION

Spectral editing is a very useful technique for simplifying complex spectra and for assigning signals of chemically distinct nuclei in high resolution NMR. In liquid ^{13}C NMR spectroscopy, editing techniques, such as DEPT, INEPT and APT (1), are commonly used. Although CP/MASS (2-4) has been in routine use for more than twenty years, very few spectral editing methods have been developed which can be applied to rigid solids.

One of the most routinely used techniques for spectral editing in CP/MASS is the delayed decoupling (or dipolar dephasing) sequence (5). Unfortunately, this technique does not clearly distinguish between methine and methylene groups. To distinguish ^{13}CH and $^{13}CH_2$ signals, several other schemes have been proposed (6-10). Most of them, such as the two-dimensional Separated Local Field (SLF) experiments (2DSLF)(6,7), a one-dimensional adaption of SLF (1DSLF) (8), are based purely on the fact that a $^{13}CH_2$ group has two ^{13}C-^{1}H dipolar couplings and a ^{13}CH group only one. Usually $^{13}CH_3$ groups are treated as nonprotonated carbons as their ^{13}C-^{1}H dipolar couplings are effectively removed by rapid methyl group rotations. In fact, the ^{13}C-^{1}H coupling intensity is sensitive to molecular motion, resulting in some ambiguity in the results using these approaches. A recently proposed scheme, windowless isotropic mixing for spectral editing (WIMSE)(10) and most of the others mentioned above require the application of multiple-pulse techniques in at least one of the RF channels. Synchronization of the sample spinning with the cycle time of the multiple-pulse sequences is also necessary in many cases, restricting the selection of rotor speed and demanding its precise control.

In this paper, a simpler method for distinguishing between ^{13}CH and

$^{13}CH_2$ as well as $^{13}CH_3$ and nonprotonated carbon signals in CP/MASS is proposed. It makes use of the fact that not only are the cross relaxation (CR) rates for all these groups different, but so to are the ratios of the heat capacities of the two sorts of spins during the CR for the ^{13}CH and $^{13}CH_2$ groups (11). Since the characteristic ratio of the heat capacities is independent of the molecular motion, the new approach is more reliable in some instances. The pulse sequence used is the polarization inversion (PI) sequence (12-14), which is a simple modification of the standard CP method. The instrumental set-up is the same as in the routine CP/MASS experiment. As a result, this method is very easy to apply.

In the following, the spin dynamics of polarization inversion at both low (or moderate) and high MASS speeds will be described. A powder sample of fumaric acid monoethyl ester was chosen as a model sample to study the spin dynamics and to test the editing technique. The new approach was then applied to sucrose, polystyrene and cholesteryl acetate. Sucrose has eight CH groups and three CH_2 groups making it an ideal test sample. Polystyrene was chosen as a representative polymer (7,10). Cholesteryl acetate is a small biomolecule with a complex ^{13}C CPMAS NMR spectrum, where the peak assignment is not straightforward (7).

THEORY

The technique used in this work is the standard cross polarization (CP) sequence combined with polarization inversion (PI) as diagrammed in Fig. 1. Under the Hartmann-Hahn condition, $\gamma_{1I}B_{1I} = \gamma_{1S}B_{1S}$, the S magnetization M_S is created gradually as the cross polarization time τ_{cp} is increased. After a sufficiently long τ_{cp}, the S and I spins reach a common spin temperature. If the phase of the I spin channel is then shifted by 180^0, the spin temperature of the I spins is inverted. The I and S spin systems are no longer at thermal equilibrium and energy transfer occurs again until a new common spin temperature is reached. As the polarization inversion time τ_{pi} increases, the S magnetization decreases at first, passes through zero, and finally becomes negative. This process has been named polarization inversion (14) and has the same spin dynamics as the standard cross polarization (15).

For an S-I spin pair in a stationary sample, the energy is transferred back and forth between the directly bonded S and I spins with a frequency determined by the S-I coupling intensity (16). As a result, the S magnetization oscillates during the cross relaxation process. The homonuclear dipolar couplings among the I spins transfer the polarization between the spin pair and the other I spins, and dampen the oscillation. A quantitative expression for the polarized S magnetization M_{SX} in the standard CP experiments on a single crystal sample has been given by Müller et al. (16):

$$M_{SX} = M_{\infty} \left\{ 1 - \frac{1}{2} \exp(-R\tau_{cp}) - \frac{1}{2} \exp\left(-\frac{3R\tau_{cp}}{2}\right) \cos\left(\frac{b\tau_{cp}}{2}\right) \right\} \quad [1]$$

In equation 1 b is the dipolar coupling intensity, R is the spin diffusion

rate among protons, and τ_{cp} is the cross polarization time.

Under MASS, the contributions from all of the magnetically equivalent S spins with different orientations will add to form a single narrow line or a center band flanked by sidebands. The oscillations with different frequencies destructively interfere with each other, resulting in a rapid decay. It turns out that the S magnetization, as a function of the CP time τ_{Cp}, can be approximately expressed as (11):

$$M_{SX} = M_{\infty} \left\{ 1 - \frac{1}{2} \exp\left(-R\tau_{cp}\right) - \frac{1}{2} \exp\left(-\frac{3R\tau_{cp}}{2}\right) \exp\left(-\frac{\tau_{cp}^2}{T_{SI}^2}\right) \right\} \quad [2]$$

where

$$\left(\frac{2}{T_{SI}^2}\right) = \frac{\sum_i I_i \left(\frac{b_i}{2}\right)^2}{\sum_i I_i} \quad [3]$$

and the summation is over the all possible orientations. For typical organic compounds, the spin diffusion time constant R^{-1} is several hundreds of μs, while T_{SI} is tens of μs (17). Thus for rigid SI_n groups, cross polarization is not a single exponential process, but proceeds in two stages with quite different time constants. The S magnetization increases rapidly during the first tens of μs, then approaches the equilibrium value at a much slower rate.

It has been shown that the spin dynamics in the polarization inversion process is essentially the same as in the standard cross polarization experiment (15). In the PI experiment of a stationary sample, the S magnetization, as a function of the cross relaxation time, oscillates with the same frequency and the same dampening as in CP. The only difference is the initial condition. It is easy to deduce a formula describing the S signal intensity as a function of the polarization inversion time τ_{pi}:

$$M_{SI} = M_{SI}^{0} \left\{ \exp\left(-R\tau_{pi}\right) + \exp\left(-\frac{3R\tau_{pi}}{2}\right) \exp\left(-\frac{\tau_{pi}^{2}}{T_{SI}^{2}}\right) - 1 \right\} \quad [4]$$

where M_{SI}^{0} is the signal intensity just before polarization inversion. Equation 4 tells us that the ^{13}CH signal rapidly decreases to zero during the first tens of μs, then approaches $-M_{SI}^{0}$ slowly.

A similar process can be analyzed for an SI_2 group (11). There are two I spins that are directly bonded to an S spin. Thus in the fast PI stage, the opposite polarizations do not cancel each other completely. The surviving polarization is shared equally by the three spins. Consequently, at the end of the fast PI stage, the residual S magnetization for the SI_2 groups is $(-M_{SI_2}^{0}/3)$. It turns out that the expression for the S magnetization is:

$$M_{SI_2} = M_{SI_2}^{0} \left\{ \frac{2}{3} \exp\left(-R\tau_{pi}\right) + \frac{4}{3} \exp\left(-\frac{3R\tau_{pi}}{2}\right) \exp\left(-\frac{\tau_{pi}^{2}}{T_{SI_2}^{2}}\right) - 1 \right\} \quad [5]$$

The initial PI rate $T_{SI_2}^{-1}$ is faster than T_{SI}^{-1} due to the two ^{13}C-^{1}H heteronuclear couplings. Because the PI rates of the two stages are significantly different, there is a sharp turning point in the polarization inversion curve, which is a plot of the S signal intensity versus polarization inversion time τ_{pi}. Thus the choice of the actual polarization inversion time needed for observing the residual signal intensities at the turning point of the two stages is not critical. For methyl and nonprotonated carbons, the CR process is nearly exponential. The CR rate for a nonprotonated carbon is the slowest one. Both can be easily recognized.

These arguments are true only under the Hartmann-Hahn condition. Under

mismatched conditions, although the initial CR rate does not change, only a portion of the SI_n subsystems can take part in a rapid polarization transfer (18-20). As a result, a portion of the ^{13}CH units do not undergo cancellation of their magnetizations during the first PI stage, resulting in a noticeable positive signal intensity. For $^{13}CH_2$ units, the residual signal may have much smaller amplitude and may even have positive intensity.

This problem can be solved by simultaneously inverting the phases in the two RF channels during the polarization inversion process (18,20,21). As shown in Figure 1b, instead of a single τ_{pi} with fixed phases in the two channels, the polarization inversion time is divided into two parts , τ_{pi1} and τ_{pi2}. The phases during τ_{pi1} are the same as during τ_{pi} in the Fig. 1a, while the phases during τ_{pi2} are inverted in both channels. If the mismatch of the Hartmann-Hahn condition, $|\omega_{1I}-\omega_{1S}|$, is not very large, the simultaneous phase inversion forces all the rigid SI_n subsystems to undergo a rapid polarization transfer, as in a perfectly matched condition (20).

The above analysis is correct at low or moderate MASS speeds (for example, < 5 kHz) for typical organic compounds. At high MASS speed, for example, at 10 kHz, the proton-proton dipolar coupling is suppressed to some extent. The resulting cross relaxation dynamics are quite different (22). The subsystems SI_n behave as though they are isolated from the other I spins.

For an isolated SI spin pair, the time-dependent heteronuclear coupling is:

$$\mathcal{H}_{SI}(t) = 2b(t)I_zS_z \quad . \qquad [8]$$

Here

$$b(t) = \sum_{k=-2}^{2} b_k \exp(ik\omega_r t), \qquad [9]$$

with

$$\left.\begin{aligned} b_0 &= 0 \\ b_{\pm 1} &= \frac{\gamma_I \gamma_S \hbar^2}{r^3} \frac{\sqrt{2}}{4} \sin(2\beta) \exp(\pm i\gamma) \\ b_{\pm 2} &= \frac{\gamma_I \gamma_S \hbar^2}{r^3} \frac{1}{4} \sin^2\beta \exp(\pm 2i\gamma) \end{aligned}\right\} \qquad [10]$$

The angles β and γ specify the orientation of the z axis of the SI dipolar coupling tensor in the spinner-fixed frame (23).

After an integral number of rotor periods, the average coupling becomes zero

$$\bar{\mathcal{H}}_{SI} = 0, \qquad [11]$$

so that the net polarization transfer disappears. For the polarizarion inversion experiments, the S magnetization of the SI groups recovers its full amplitude at each integral number of rotor periods.

For SI_2 groups however, the behavior is different. The two I spins couple to each other strongly due to the short interspin distance. This I-I coupling intensity is about 35 kHz in size so that it is hardly suppressed by 10 kHz MASS. The coupling for the SI_2 subsystem is:

$$\mathcal{H}_{SI_2}(t) = 2b_1(t)I_{z1}S_z + 2b_2(t)I_{z2}S_z + 2b_{12}(t)(3I_{z1}I_{z2} - \vec{I}_1 \cdot \vec{I}_2) \qquad [12]$$

This Hamiltonian $\mathcal{H}_{SI_2}(t)$ is thus homogeneous; i.e., $\mathcal{H}_{SI_2}(t)$ does not commute with itself at different times (24). Although its zeroth-order average is zero, the higher order corrections to the average Hamiltonian $\bar{\mathcal{H}}_{SI_2}$ are not zero. The S magnetization of the SI_2 groups will form weak echoes at only

the first few rotor periods, and the longer the PI time, the smaller the recovery. In fact, as the subsystems SI_n are not completely isolated at 10 kHz MASS, there is still additional dampening due to the residual coupling to the other I spins. The refocussing of the SI signal is thus not complete. However, the difference between SI and SI_2 signals is still obvious.

With high speed MASS, it has been found that the most efficient cross relaxation occurs under the conditions (22) :

$$\Delta\omega = (\omega_{1I} - \omega_{1S}) = \pm (1 \text{ or } 2)\omega_r, \qquad [13]$$

where ω_r is the rotor speed. However, to get a large echo from a ^{13}CH group in PI experiments, the RF strengths have to be set at the condition $\Delta\omega = 0$. The reason for this is that the mismatched Hartmann-Hahn condition introduces another time-dependent factor into the heteronuclear coupling, resulting in a time-independent component. The detailed cross relaxation dynamics under high speed MASS conditions have been described in Ref. 25. Here only a brief analysis is given. After transforming to the toggling frame defined by

$$A^T = \exp(-i\omega_{1I}I_x - i\omega_{1S}S_x)t \; A \; \exp(i\omega_{1I}I_x + i\omega_{1S}S_x)t \qquad [14]$$

the heteronuclear coupling becomes:

$$H_{SI}(t)^T = 2b(t) \times \left\{ \begin{array}{l} I_z S_z [\cos(\omega_{1I}+\omega_{1S})t + \cos(\omega_{1I}-\omega_{1S})t] \\ + I_y S_y [-\cos(\omega_{1I}+\omega_{1S})t + \cos(\omega_{1I}-\omega_{1S})t] \\ + I_y S_z [\sin(\omega_{1I}+\omega_{1S})t - \sin(\omega_{1I}-\omega_{1S})t] \\ + I_z S_y [\sin(\omega_{1I}+\omega_{1S})t + \sin(\omega_{1I}-\omega_{1S})t] \end{array} \right\} \qquad [15]$$

When $\Delta\omega = \pm (1 \text{ or } 2)\omega_r$, the terms $b(t)\cos(\Delta\omega t)$ and $b(t)\sin(\Delta\omega t)$ give several time-independent components. As a result, the average coupling for an SI pair is no longer equal to zero after an integral number of rotor periods and an echo does not appear.

EXPERIMENTS

Experiments were performed on a homebuilt NMR spectrometer controlled by a Tecmag data system and using an Oxford instrument 7.05 T, 89-mm room-temperature bore superconducting solenoid. Both RF channel levels, $\omega_{1I}/2\pi$ and $\omega_{1S}/2\pi$, were set to about 50 kHz. The proton RF strength of X phase is fixed. The S channel RF strength can be finely adjusted by using an in-line attenuator with the smallest step of 0.1 db so that the (-X) phase of the S channel can be well matched to the X phase of the I channel. After the S channel RF strength is fixed, the (-X) phase of the I channel can be independently adjusted so that both periods of PI time, τ_{pi1} and τ_{pi2}, can be under the Hartmann-Hahn condition.

Both low speed and high speed Doty CP MASS probes have been used. The MASS speed is controlled by changing the air pressure which drives the spinner and is stabilized by using two standard air pressure regulators. The fluctuation of MASS speed at 5~10 kHz is smaller than 50 Hz over several hours.

RESULTS

The polarization inversion (PI) curves display the S signal intensity versus the polarization inversion time τ_{pi}. Figure 2a shows the PI curves for the ^{13}CH, $^{13}CH_2$, $^{13}CH_3$ and nonprotonated ^{13}C of fumaric acid monoethyl ester at 5 kHz MASS. The pulse sequence used is shown in Fig. 1a. There is no simultaneous phase inversion during PI. As τ_{pi} is increased, the normalized S signal intensity changes from 100% to -100%. The PI curves during the first 600 μs are expanded in the Fig. 2b. The two-stage feature

of the cross relaxation for the rigid protonated S signals is obvious. The polarization inversion time when the S signal becomes zero can be used as a rough estimate of the PI rate. This time is 25, 40, 110 and 350 μs for $^{13}CH_2$, ^{13}CH, $^{13}CH_3$ and nonprotonated ^{13}C groups respectively. The $^{13}CH_2$ and ^{13}CH signals do not monotonically change in time. For example, a minimum appears at τ_{pi} = 80 μs for the ^{13}CH curve, which is different from the prediction of Eq. 4 . The reason is that polarization transfer is actually an oscillating process. The oscillations do not disappear when the sample is spun, although they desctructively interfere each other. As a result, there is an apparent oscillation with very small amplitude remaining around the turning point of the PI curve. In spite of this small deviation, Eqs. 4 and 5 describe the overall features, especially the two-stage behavior, of the PI process very well. In the range of τ_{pi} from 60 to 200 μs, the ^{13}CH signal fluctuates between -10% to -20%, while $^{13}CH_2$ signal is between -40% to -50%. Identification of these two kinds of signals is straightforward.

Table 1 shows the effects of the Hartmann-Hahn match conditions and the simultaneous phase inversion during the PI time. The experimental conditions are otherwise the same as above. When the deviation of the Hartmann-Hahn condition is 10%, the residual ^{13}CH signal is quite large, up to 22%, while the $^{13}CH_2$ signal has a very small negative amplitude. Under such a large mismatch condition, the simultaneous phase inversion is very effective, resulting in a spectrum similar to that under a matched condition.

Spectra of fumaric acid monoethyl ester obtained by using cross polarization combined with polarization inversion (CPPI) are displayed in Fig. 3. Two different PI times were used; $\tau_{pi1} = \tau_{pi2}$ = 20 μs (middle) and 45 μs (bottom). For comparison, the standard CP/MASS spectrum is also

displayed (top). In the CPPI/MASS spectra, the ^{13}CH center band at 130 ppm and its sideband almost disappear. The methylene line at 60 ppm is inverted with a relative intensity of 30.6% and 34.0%, respectively, in the two cases. The nonprotonated ^{13}C signals at 160 and 170 ppm are the least affected. When $\tau_{pi1} = \tau_{pi2} = 20$ μs, the nonprotonated ^{13}C and $^{13}CH_3$ (at 15 ppm) signal intensities reduce to 85 % and 47 %, respectively.

The PI curves at 10 kHz MASS for fumaric acid monoethyl ester are shown in Figure 4a. The first 400 μs region is expanded in Fig. 4b. The PI process occurs under the Hartmann-Hahn condition. At the end of the first rotor period, $\tau_{pi} = 100$ μs, each signal has a large rotational echo. However, at the end of the second period, a significant rotational echo appears only for ^{13}CH. The nonprotonated ^{13}C and the methyl carbon are weakly coupled to several protons so that the coupling behaves more homogeneously. At $\tau_{pi} = 200$ μs, the ^{13}CH has a relative intensity of 35%, while that for the $^{13}CH_2$ is ~25%. The CR rate for the nonprotonated ^{13}C is very small (25) so that its signal intensity is virtually unchanged. The $^{13}CH_3$ signal intensity reduces to 60%.

Figure 5 compares the PI curves for ^{13}CH signal of fumaric acid monoethyl ester at 10 kHz MASS under a matched and a mismatched condition. No rotational echo occurs under the mismatched condition.

The CP/MASS and CPPI/MASS spectra of sucrose are shown in the middle and on the bottom of Fig. 6, respectively. The MASS speed was 3.5 kHz. When $\tau_{pi1} = \tau_{pi2} = 20$ μs, all lines become negative, except the one at highest frequency, which is a nonprotonated carbon signal. However, the relative intensity of these negative peaks is different. If the intensity of the CPPI/MASS spectrum is multiplied by 3.3 and then added to the standard CP/MASS spectrum, a PI edited spectrum is obtained. As shown at the top of

the Figure, the three $^{13}CH_2$ signals (at the lower frequency of the spectrum) disappear in the edited spectrum while the ^{13}CH signal intensity changes only slightly compared with the standard CP/MASS spectrum.

Figure 7 shows the CPPI/MASS as well as the standard CP/MASS spectra for polystyrene. There are several lines: $^{13}COOH$ at 147 ppm, ^{13}CH at 129 ppm, and overlapping ^{13}CH and $^{13}CH_2$ resonances at about 43 ppm. In the CPPI/MASS spectrum, the $^{13}COOH$ signal intensity reduces to 80 %, that of the ^{13}CH centerband reduces to 6 %, while its sidebands become negative (vide infra). At 44 ppm, a negative peak appears for a $^{13}CH_2$ line. The PI edited peak at 42 ppm is shown at the upper-right corner of Fig.7. This peak contains primarily ^{13}CH resonances. It has a relative intensity of 45.7 % with respect to the overlapping peak of the CP/MASS spectrum, which is consistent with the known fact that the broad peak at 44 ppm results from overlap of a ^{13}CH peak and a $^{13}CH_2$ peak. This result shows that spectral editing using PI combined with SPI can be useful as a semi-quantitative method.

The 4.7 kHz CP/MASS spectrum for cholesteryl acetate in the top of figure 8 is quite complex and displays many more resonances than there are carbons in the molecule. Since the unit cell contains two crystallographically nonequivalent molecules, there are pairs of lines of equal intensity in the spectrum (26). The shift differences between the pairs of lines are not uniform. They are largest at the positions closest to the magnetically anisotropic ester and alkene functionalities (7). At the bottom of Fig. 8, the CPPI/MASS spectrum obtained with $\tau_{pi1} = \tau_{pi2} = 20$ μs is displayed. The number of the scans for the CPPI/MASS spectrum is three times of that for the CP/MASS spectrum. Thus the actual intensity of the CPPI/MASS spectrum is one third of that displayed. As shown in Fig. 8,

the $^{13}CH_2$ peaks are easy to identify, since they have nearly the same amplitude and an opposite polarization in the two spectra. In addition, as the CPPI/MASS spectrum has a weaker intensity, it is necessary to increase the number of scans to improve the signal/noise ratio.

It is easy to recognize that the signals at about 140 and 168 ppm are nonprotonated, while those at about 51, 57, 73, and 122 ppm are ^{13}CH (●). Other peaks from 45 to 170 ppm are sidebands. Spectral overlap in the aliphatic region is fairly severe. An expansion of the 10-45 ppm region is shown in Fig. 9. In the middle is the standard CP/MASS spectrum, on the bottom is the CPPI/MASS result, while at the top is the PI edited spectrum. Many assignments can be made by inspection. In particular, ^{13}CH signals are clearly displayed in the PI edited spectrum even when they overlap with $^{13}CH_2$ lines in the CP/MASS spectrum. There is no ambiguity in assigning the peaks at 27.0, 27.6, 30.0, 32.9, and 38.6 ppm to $^{13}CH_2$ groups (□), the peaks at 28.9, 32.1, and 39.4 ppm to ^{13}CH (●). The peaks at 28.5, 40.7 and 41.4 ppm are overlapping $^{13}CH_2$ and ^{13}CH signals. The pair of lines at about 13 ppm are due to $^{13}CH_3$, and the pairs at 42.2 and 42.9 ppm correspond to nonprotonated carbon signals. The pair of lines at about 36.5 and 37.5 ppm are obviously overlapping nonprotonated carbon and $^{13}CH_2$ signals, since on the bottom of Fig. 9, the linewidths of the positive signals are much narrower and a negative peak appears. The overlap of the lines in the region 17-26 ppm is more severe. The coupling strength for $^{13}CH_3$ has a wide distribution due to the different degrees of the rotational motion (27). As a result, after PI the $^{13}CH_3$ signals may be attenuated differently. The methylene lines are quite broad. All these facts add more difficulties to the line assignment. However, some conclusions can be drawn. The relative intensities of the signals at about 18.6, 18.8, 19.5,

and 20.8, are reduced to nearly the same amount as that at 13 ppm, being about 60%. They are certainly $^{13}CH_3$ signals. At 21.5 and 25.1 ppm, negative peaks appear, indicating the existence of $^{13}CH_2$ signals. According to Roberts' solution assignment (28), there are five methyls and three methylenes in the region 17-26 ppm. The $^{13}CH_3$ signals at 21.8, 22.2, 24.6 and 25.4 ppm are reduced slightly more after PI, which is due to overlap with $^{13}CH_2$ signals. The signals at 22.9, 23.7 ppm are less attenuated, indicating more freedom of motion. Taking into account that there are significant chemical-shift differences of various carbons between the solution and solid state (8), our analysis is basically consistent with Roberts' assignment.

DISCUSSION

Compared with other schemes, this spectral editing method for solids has some advantages. First, it is very simple. No adjustments of the instrument other than those for routine CP/MASS are required. Since multiple pulse irradiation is not applied, accurate control and stabilization of the MAS rate for pulse sequence synchronization is not required (8,10). In some multiple pulse based techniques only rather slow rotor speeds can be used. In contrast, spectral editing using PI is unrestricted in this regard. By using SPI, the requirement of a well matched Hartmann-Hahn condition is also relaxed.

The PI spectral editing technique is also inherently more reliable than methods which depend upon the size of ^{13}C-^{1}H dipolar couplings. Molecular motions may significantly influence the strengths of dipolar couplings. All spectral editing methods then that are based purely on the different

coupling intensities of different groups will be sensitive to such molecular motions. In contrats the ratio of the heat capacities between the S and I spins in the SI_n subsystem is basically equal to the ratio of the numbers of the two spins, which is independent of the molecular motion. While molecular motions may average the heteronuclear couplings, same motions usually will attenuate the homonuclear couplings among the abundant I spins as well. Consequently, the cross relaxation process for ^{13}CH or $^{13}CH_2$ units may maintain its two-stage character and the spectral editing method proposed in this paper will still provide useful results. Only when molecular motion is so great that intramolecular dipolar couplings are averaged to zero and CP is accomplished by intermolecular dipolar interactions will this method fail. Under these conditions, however, J couplings may be used to edit the lines (29). Further work is required to check the limitations.

The spectral editing of methine and methylene carbon signals using the polarization inversion has been mentioned by other authors (14,30). However, the underlying principles and the methods that we have proposed are different. In the previous work, it was mentioned that cross relaxation is a single-exponential process. Due to the different coupling intensities exerted on the ^{13}C nuclei in ^{13}CH and $^{13}CH_2$ groups, the CP rate is faster for $^{13}CH_2$ groups than for ^{13}CH. As a result, nulling of the methylene carbon signals requires a shorter polarization inversion time. Hartmann et al (30) used the term "cross-depolarization" instead of "polarization inversion" as used in our paper. In addition to PI, Hartmann et al have introduced cross-repolarization. By suitable choice of the polarization inversion and repolarization times, selective nulling of methine or methylene carbon signals is possible. However, a suitable choice of the two

cross relaxation times may be not easy. It may vary from sample to sample as mentioned by Hartmann et al. It also depends on the actual match conditions of ω_{1I} and ω_{1S}. In contrast, the method we have presented is much less sensitive to the cross relaxation rates and the match conditions. For example, for low to moderate MASS rates, methine and methylene groups in typical organic compounds are easy to identify in the whole range of τ_{pi} = 40 - 200 μs.

There are some distortions in CPPI/MASS spectra that merit discussion. For example, the PI edited peak shown in the corner of Fig. 7 should be the ^{13}CH signal. However, the line shape is not a perfect Lorentzian type. It seems that different portions of the SI_n line have slightly different effective cross relaxation rates so that the line shape is different before and after the short PI time. The distortion is more obviously displayed in the sidebands of the ^{13}CH line at 190 ppm. The center of gravity of this line is significantly shifted due to the PI process. Furthermore, the residual ^{13}CH centerband at 129 ppm is positive, while the corresponding sidebands at 69 and 190 ppm are both negative. The distortion originates from the fact that the effective heteronuclear coupling intensity is orientation dependent, and molecules with a different orientations in the rotor fixed frame contribute to different portions of the spectrum. It is apparent that such distortions are very small in the case of fumaric acid monoethyl ester, while they are much larger for the polystyrene spectra. Further work is required to clarify the reason for this difference. However, this kind of distortion does not inhibit the ability of the method to distinguish between methine and methylene carbon signals.

It has been mentioned that, in depolarization experiments (11), the turning point of the two CR stages occurs when $M_{SI} \sim (1/2)M_{SI}^0$ for ^{13}CH

groups and $M_{SI_2} \sim (1/3)M_{SI_2}{}^0$ for $^{13}CH_2$ groups, where $M_{SI_n}{}^0$ is the signal intensity before depolarization. This feature can also be used to identify the two signals. However, discrimination of these signals using polarization inversion is easier. In particular, when ^{13}CH and $^{13}CH_2$ lines overlap, as shown in Figs 7 and 9, they are clearly separated in the PI experiment, but not in the depolarization version.

CONCLUSION

The spectral editing of CP/MASS spectra using polarization inversion is a simple and reliable. It makes complete carbon-13 line assignment of solid state CP/MASS spectra very practical. For typical rigid solids, only a single one dimensional CPPI/MASS spectrum in addition to a standard CP/MASS spectrum is required. When MASS rates smaller than 5 kHz are used, 40 μs of polarization inversion time is the optimum. However, in a wide range of τ_{pi} values (40 ~ 200 μs), the rigid methine and methylene signals are easily recognized. At high MASS speeds, the optimum PI time is equal to twice the rotor period.

ACKOWLEDGEMENTS

This work was first presented as a poster at 33rd Experimental NMR Conference, Asilomar, Califonia (March 1992). During the course of this conference the authors learned that similar work was being carried out by Jerome L. Ackerman and coworkers. Support of this work by the U. S. Department of Energy under grant DE-FG22-91PC91285 is gratefully acknowledged.

REFERENCES

1. R. R. Ernst, G. Bodenhuasen, and A. Wokaun, "*Principles of Nuclear Magnetic Resonance in One and Two Dimensions*", The International Series of Monographs On Chemistry, Oxford Univ. Press, New York, 1987.

2. S. R. Hartmann and E. L. Hahn, *Phys. Rev.* **128**, 2042 (1962).

3. A. Pines, M. G. Gibby, and J. S. Waugh, *J. Chem. Phys.* **56**, 1776(1972): *J. Chem. Phys.* **59**, 569 (1973): *Chem. Phys. Lett.* **15**, 373(1972).

4. (a) E. R. Andrew, A. Bradbury, and R. G. Eades, *Nature* **182**, 1659(1958): (b) I. J. Lowe, *Phys. Rev. Lett.* **2**, 285(1959).

5. M. Alla and E. Lippmaa, *Chem. Phys. Lett.* **37**, 260(1976).

6. E. F. Rybaczewisky, B. L. Neff, J. S. Waugh, and J. S. Sherfinski, *J. Chem. Phys.* **67**, 1231(1977)

7. G. G. Webb and K. W. Zilm, *J. Am. Chem. Soc.* **111**, 1455(1989).

8. Naresh K. Sethi, *J. Magn. Reson.* **94**, 352(1991).

9. D. L. VanderHart and G. C. Campbell, Poster MP89, *31st Experimental NMR Conference*, Asilomar, California (April 1990).

10. D. P. Burum and A. Bielecki, *J. Magn. Reson.* **95**, 184(1991).

11. X. Wu, S. Zhang, and X. Wu, *Phys. Rev.* **B37**, 9827(1988).

12. M. T. Melchior, Poster B-29, *22nd Experimental NMR Conference*, Asilomar, California (April 1981)

13. N. Zumbulyadis, *J. Chem. Phys.* **86**, 1162(1987).

14. X. Wu, S. Zhang, and X. Wu, *J. Magn. Reson.* **77**, 343(1988).

15. X. Wu and S. Zhang, *Chem. Phys. Lett.* **156**, 79(1989).

16. L. Muller, A. Kumer, T. Baumann, and R. R. Ernst, *Phys. Rev. Lett.* **32**, 1402(1974).

17. X. Wu, X. Xie, and X. Wu, *Chem. Phys. Lett.* **162**, 325(1989).

18. S. Zhang and X. Wu, *Chem. Phys. Lett.* **156**, 333(1989).

19. S. Zhang, X. Wu and M. Mehring, *Chem. Phys. Lett.* **166**, 92(1990).

20. X. Wu and K. W. Zilm, *J. Magn. Reson.* **93**, 265(1991).

21. M. H. Levitt, D. Suter, and R. R. Ernst, *J. Chem. Phys.* 84, 4243(1986).

22. E. O. Stejskal, J. Schaefer and J. S. Waugh, *J. Magn. Reson.* 28, 105(1977).

23. T. G. Oas, R. G. Griffin, and M. H. Levitt, *J. Chem. Phys.* **89**, 692(1988)

24. M. M. Maricq and J. S. Waugh, *J. Chem. Phys.* **70**, 3300(1979).

25. X. Wu and K. W. Zilm, Poster P-169, *32nd Experimental NMR Conference*, St. Louis, (April 1991).

26. P. Sawzik and B. M. Craven, *Acta Crystallogr.* **B35**, 895(1979).

27. L. B. Alemany, D. M. Grant, R. J. Pugmire, T. D. Alger, and K. W. Zilm, *J. Am. Chem. Soc.* **105**, 2133(1983).

28. H. J. Reich, M. Jautelat, M. T. Messe, F. J. Weigert, and J. D. Roberts, *J. Am. Chem. Soc.* **91**,7445(1969).

29. T. Terao, H. Miura, and A. Saika, *J. Am. Chem. Soc.* **104**, 5228 (1982).

30. J. S. Hartmann and J. A. Ripmeester, *Chem. Phys. Lett.* **168**, 219 (1990).

Table 1

Match condition	PI time	Relative intensities $(M_{SI_n}(\tau_{pi})/M_{SI_n}{}^{0})$*	
		^{13}CH	$^{13}CH_2$
$\omega_{1I} \sim \omega_{1S}$	τ_{pi} = 40 μs	0.0	-21.0
$\omega_{1I} \sim 1.1\omega_{1S}$	τ_{pi} = 40 μs	+21.9	-5.7
$\omega_{1I} \sim 1.1\omega_{1S}$	$\tau_{pi1}=\tau_{pi2}$=20 μs	+3.9	-30.7

* See Eqs. 4 and 5.

Figure Captions

Fig. 1. The pulse sequences utilized. (a) Standard CP/MASS combined with polarization inversion (CPPI/MASS). (b) simultaneous phase inversion (SPI) during the PI.

Fig. 2. Polarization inversion curves for ^{13}CH(●), $^{13}CH_2$(□), $^{13}CH_3$(Δ) and nonprotonated ^{13}C (+) signals of fumaric acid monothyl ester at 5 kHz MASS. (a) Full PI time range. (b) Expansion of the first 600 μs.

Fig. 3. CP/MASS (top) and CPPI/MASS spectra for fumaric acid monothyl ester at 5 kHz speed. The CPPI/MASS spectrum in the middle : $\tau_{pi1} = \tau_{pi2} = 20$ μs, one on the bottom : 45 μs.

Fig. 4. Polarization inversion curves for ^{13}CH(●), $^{13}CH_2$(□), $^{13}CH_3$(Δ) and nonprotonated ^{13}C(+) signals of fumaric acid monothyl ester at 10 kHz MASS under an Hartmann-Hahn match condition. (a) Full PI time range. (b) Expansion of the first 400 μs.

Fig. 5. Polarization inversion curves for ^{13}CH signal of fumaric acid monothyl ester at 10 kHz MASS under a matched (●) and a mismatched (o) Hartmann-Hahn condition. Under the mismatched condition, there is no "rotational echo".

Fig. 6. 3.5 kHz MASS spectra of sucrose. Middle: standard CP/MASS, bottom: CPPI/MASS with $\tau_{pi1} = \tau_{pi2} = 20$ μs, and top: PI edited spectrum. The PI edited spectrum is the sum of the CP/MASS spectrum and the CPPI/MASS spectrum enhanced by 3.3 times. In the edited spectrum, $^{13}CH_2$ signals disapper, while ^{13}CH signals change slightly.

Fig. 7. CP/MASS and CPPI/MASS spectra of polystyrene at 4.6 kHz speed. The latter is obtained by using SPIPI with $\tau_{pi1} = \tau_{pi2} = 20$ μs. In the upper-right corner is the PI edited peak at 42 ppm. The PI edited peak contains primarily a ^{13}CH signal.

Fig. 8. CP/MASS (top) and CPPI/MASS (bottom) spectra for cholesteryl acetate at 4.7 kHz speed with $\tau_{pi1} = \tau_{pi2} = 20$ μs. ● stands for ^{13}CH signals.

Fig. 9. Expansion between 10-45 ppm of the MASS spectra shown in Fig. 8. Middle: standard CP/MASS, bottom: CPPI/MASS, and top: PI edited spectrum. ● stands for ^{13}CH signals, □ stands for $^{13}CH_2$ signals.

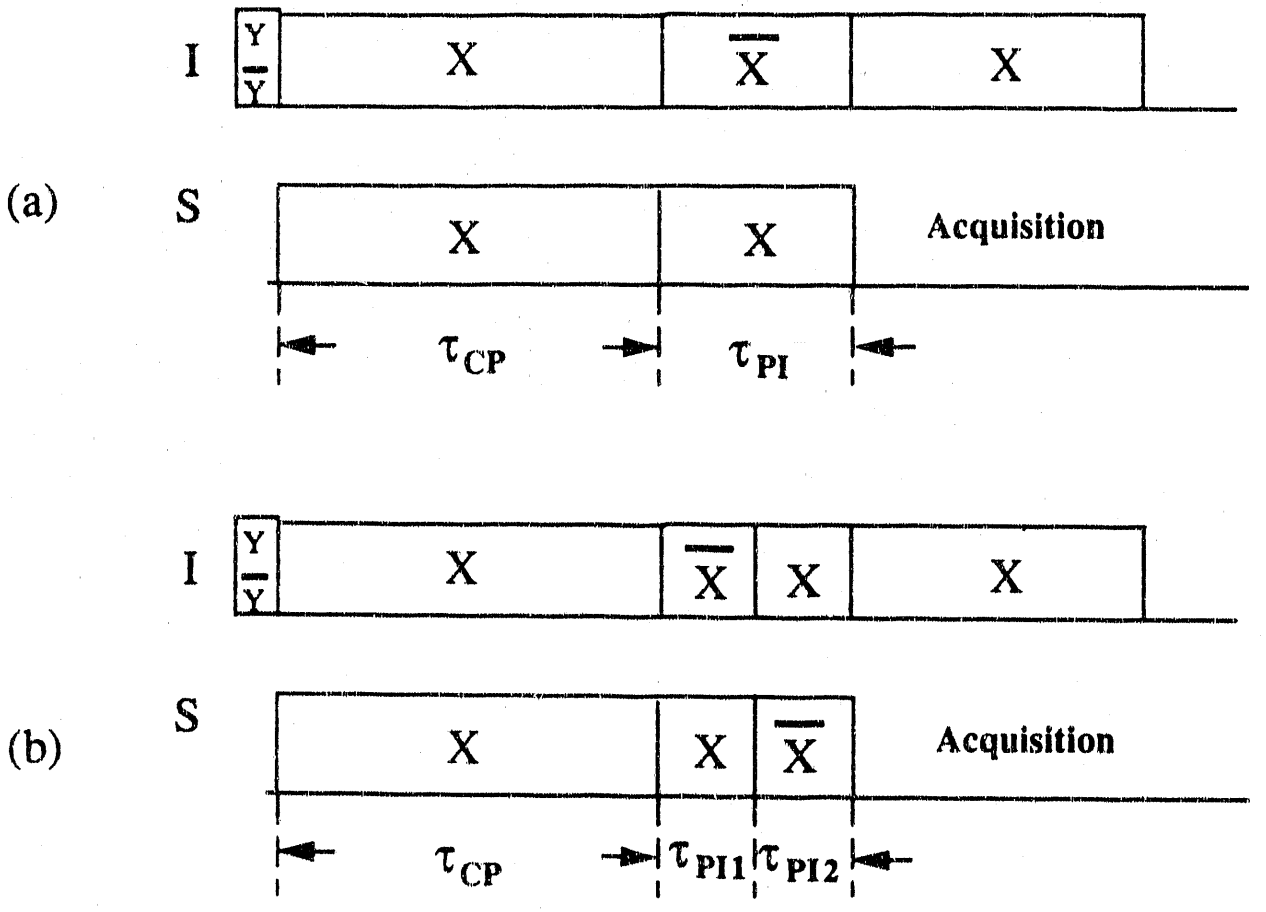
(a)
I
Y
Y
X
X
X
S
X
X
Acquisition
τ_{CP}
τ_{PI}
(b)
I
Y
Y
X
X
X
X
S
X
X
X
Acquisition
τ_{CP}
τ_{PI1}
τ_{PI2}

Figure 1

(a)

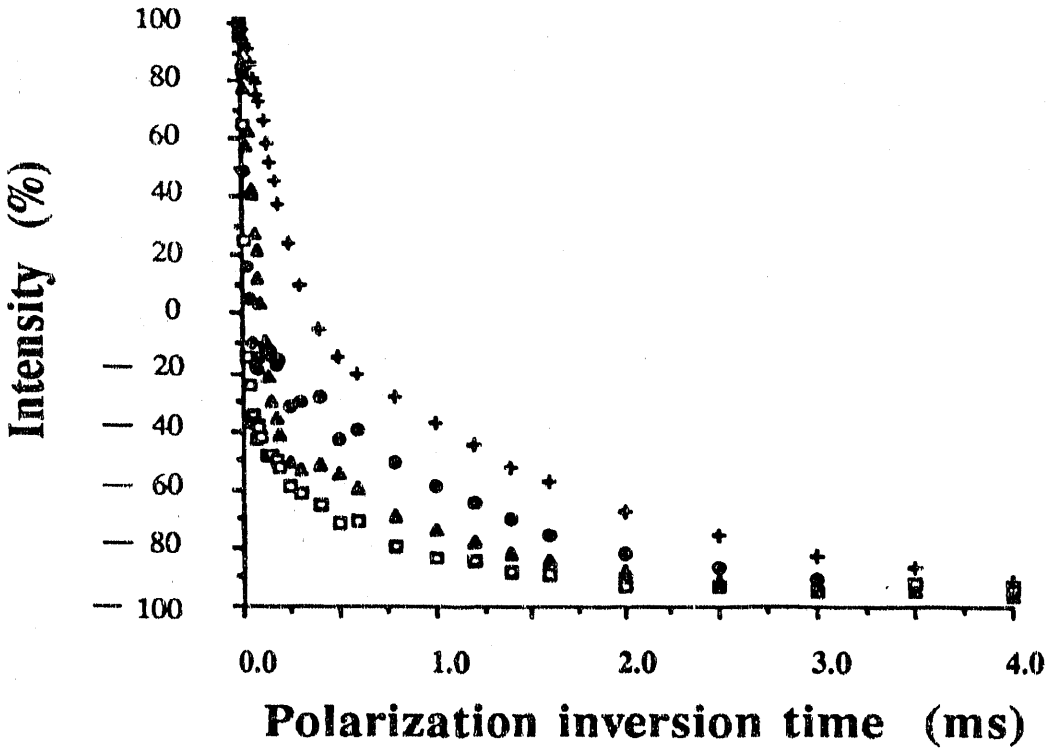
100
80
60
40
20
0
— 20
— 40
— 60
— 80
— 100
Intensity (%)
0.0
1.0
2.0
3.0
4.0
Polarization inversion time (ms)

(b)

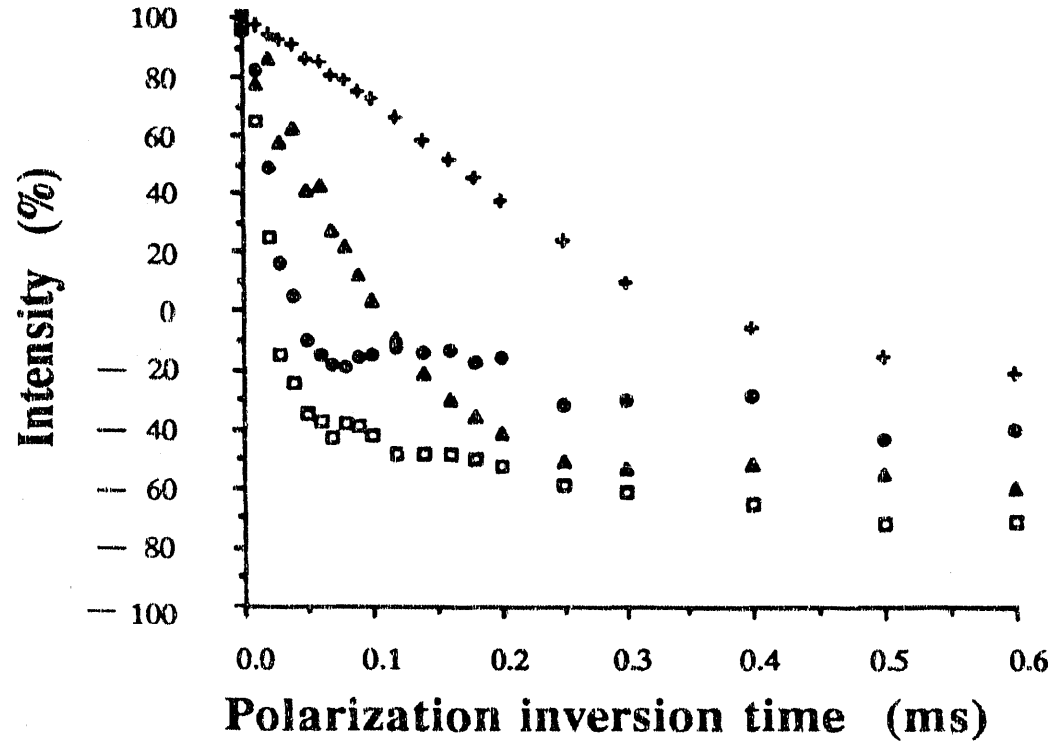
100
80
60
40
20
0
— 20
— 40
— 60
— 80
— 100
Intensity (%)
0.0
0.1
0.2
0.3
0.4
0.5
0.6
Polarization inversion time (ms)

Figure 2

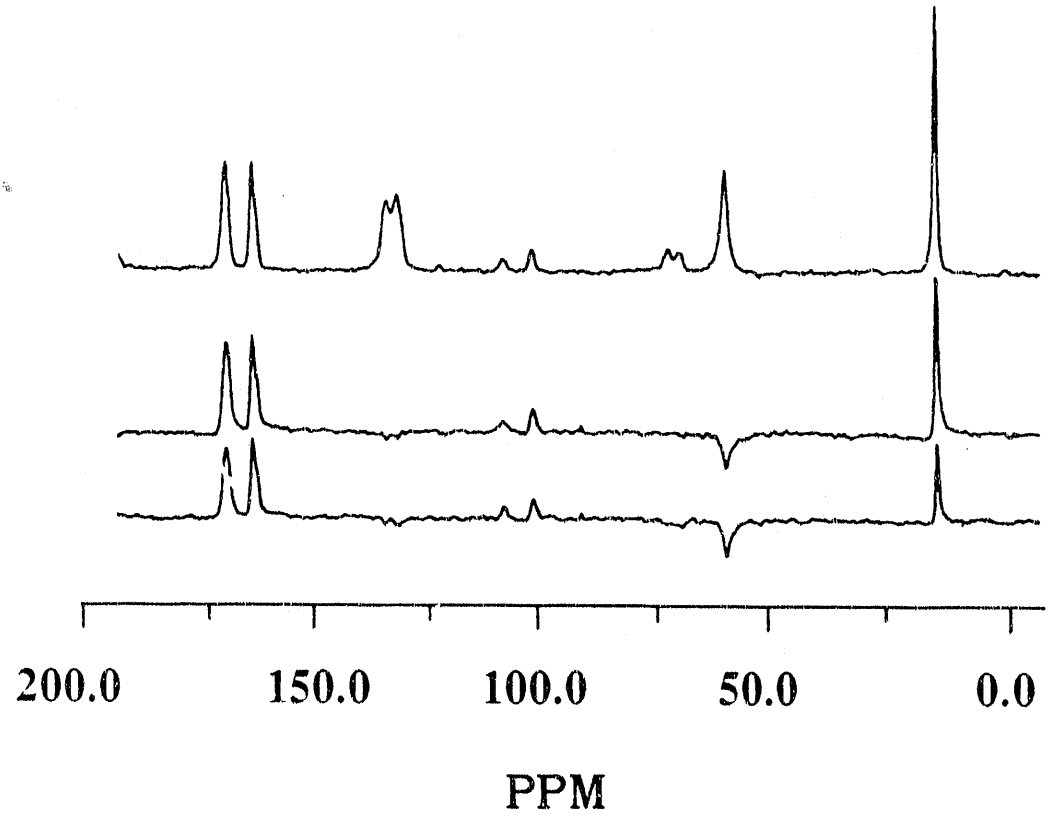

Figure 3

(a)

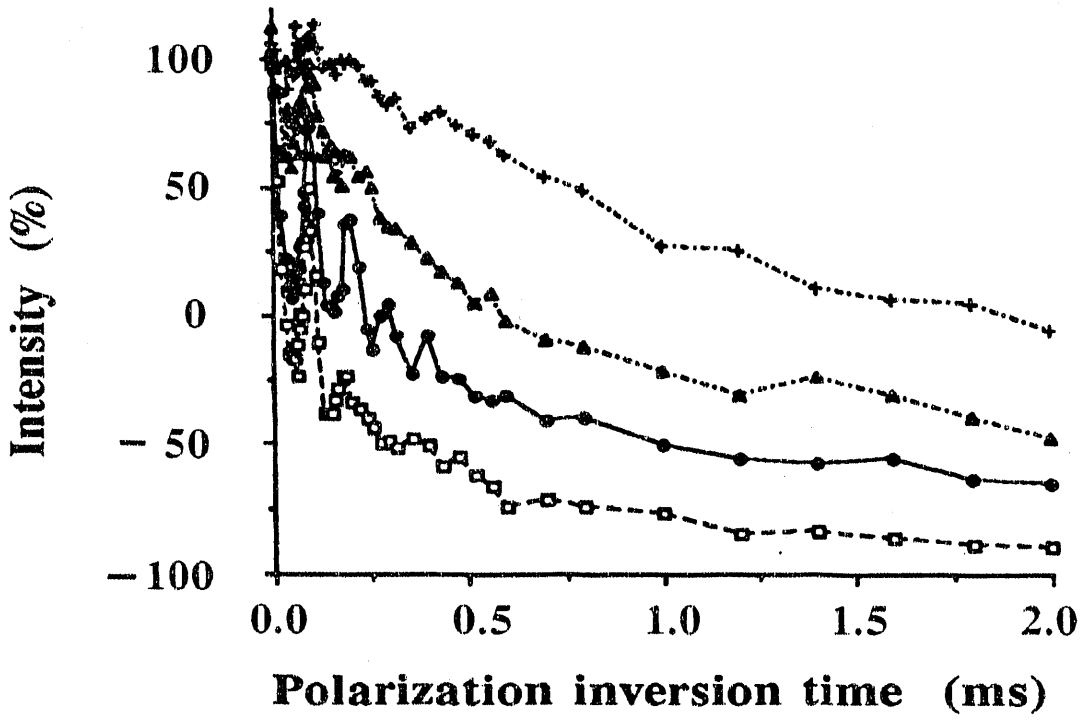
100
50
0
− 50
−100
Intensity (%)
0.0
0.5
1.0
1.5
2.0
Polarization inversion time (ms)

(b)

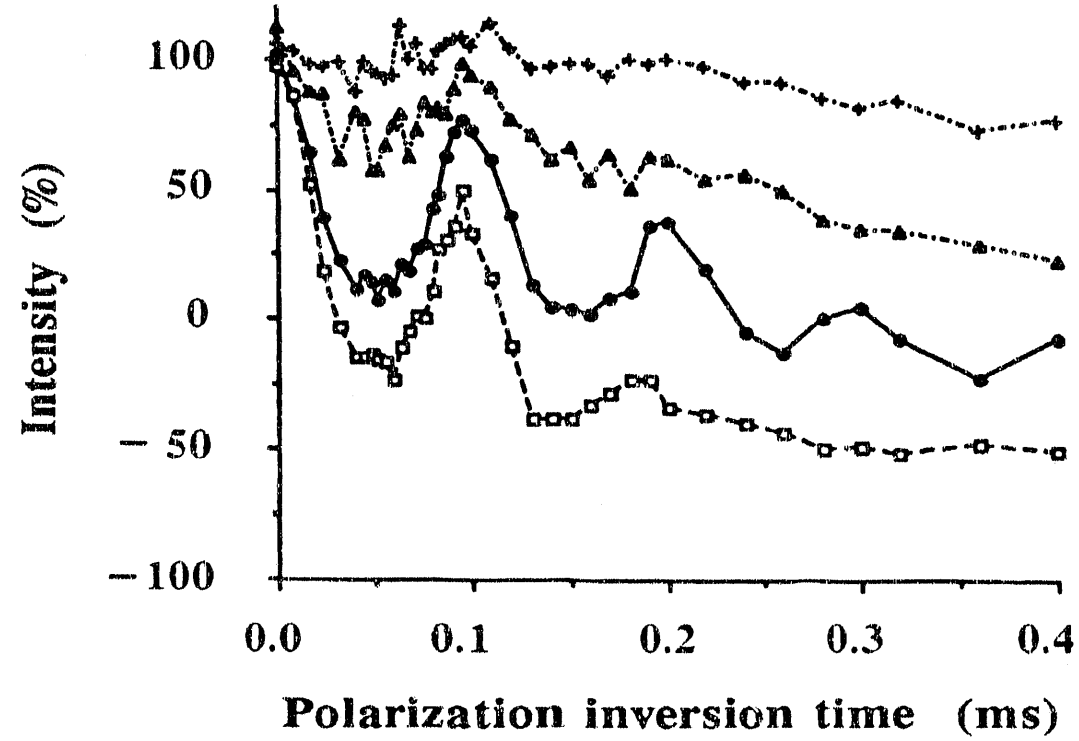
100
50
0
− 50
−100
Intensity (%)
0.0
0.1
0.2
0.3
0.4
Polarization inversion time (ms)

Figure 4

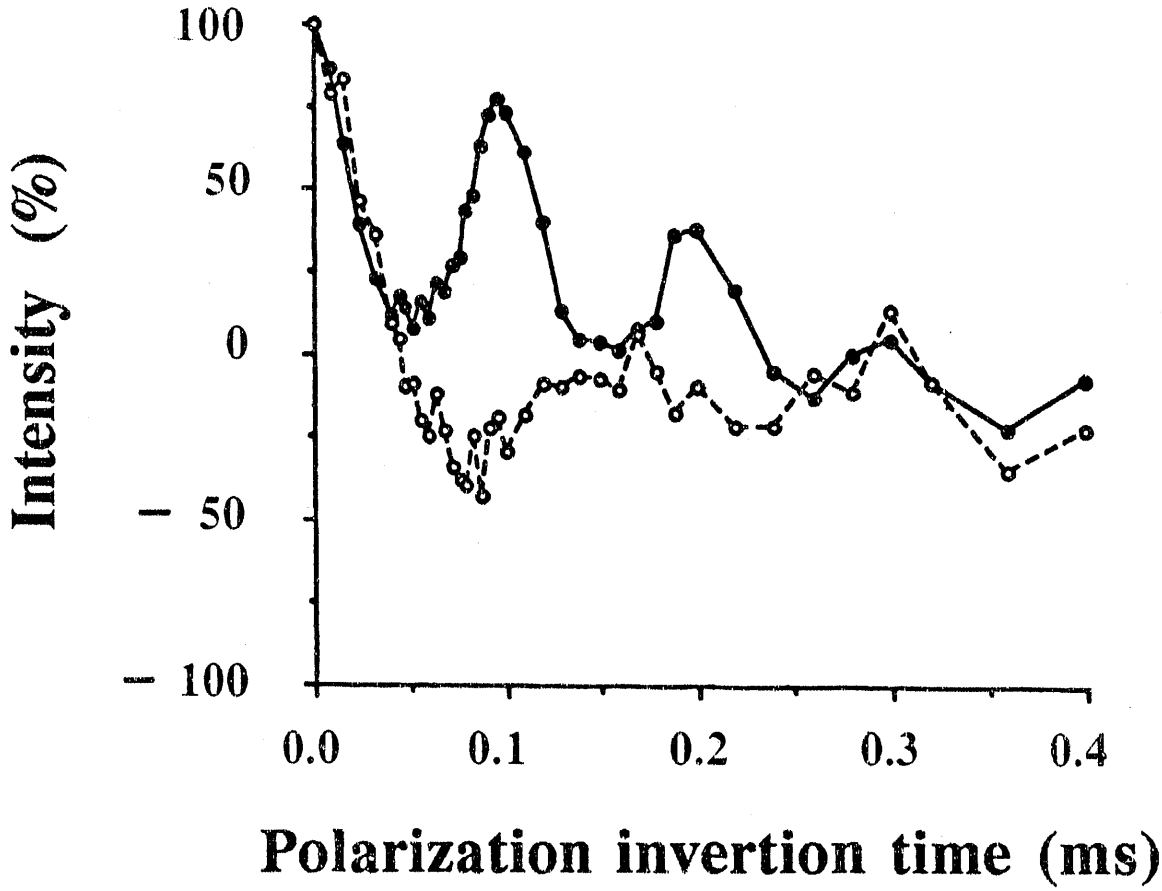
100
50
0
− 50
− 100
Intensity (%)
0.0
0.1
0.2
0.3
0.4
Polarization invertion time (ms)

Figure 5

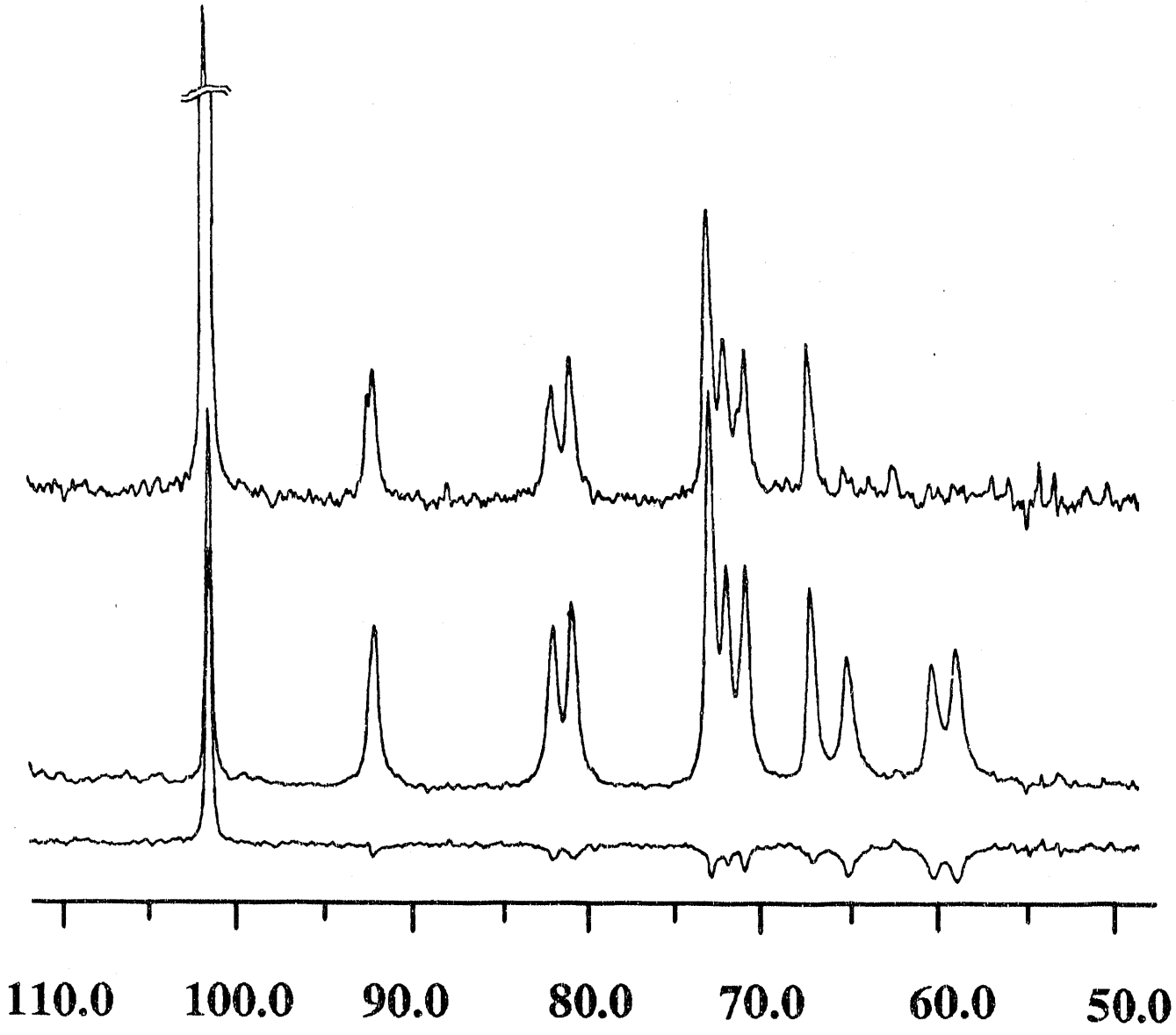

Figure 6

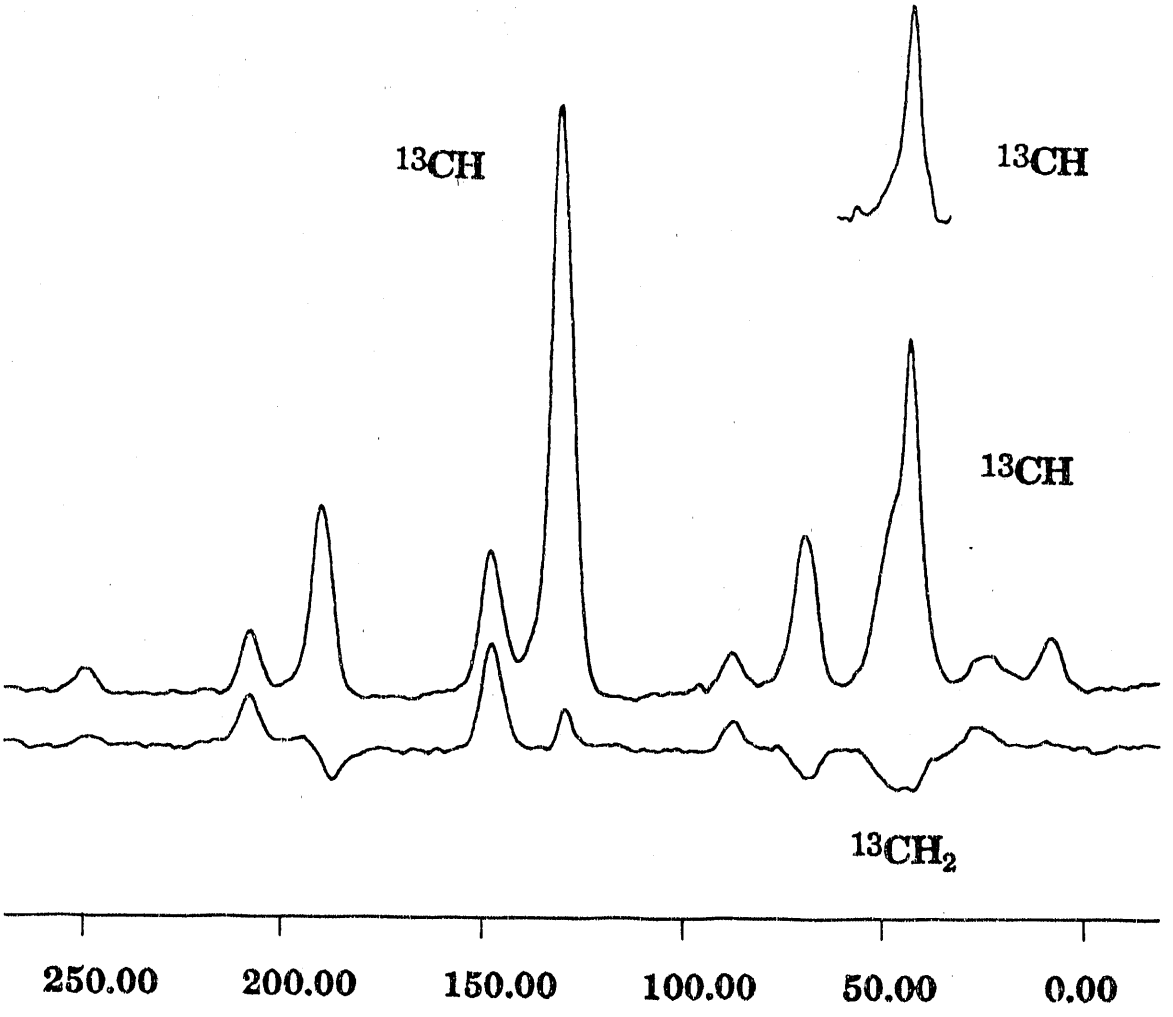

Figure 7

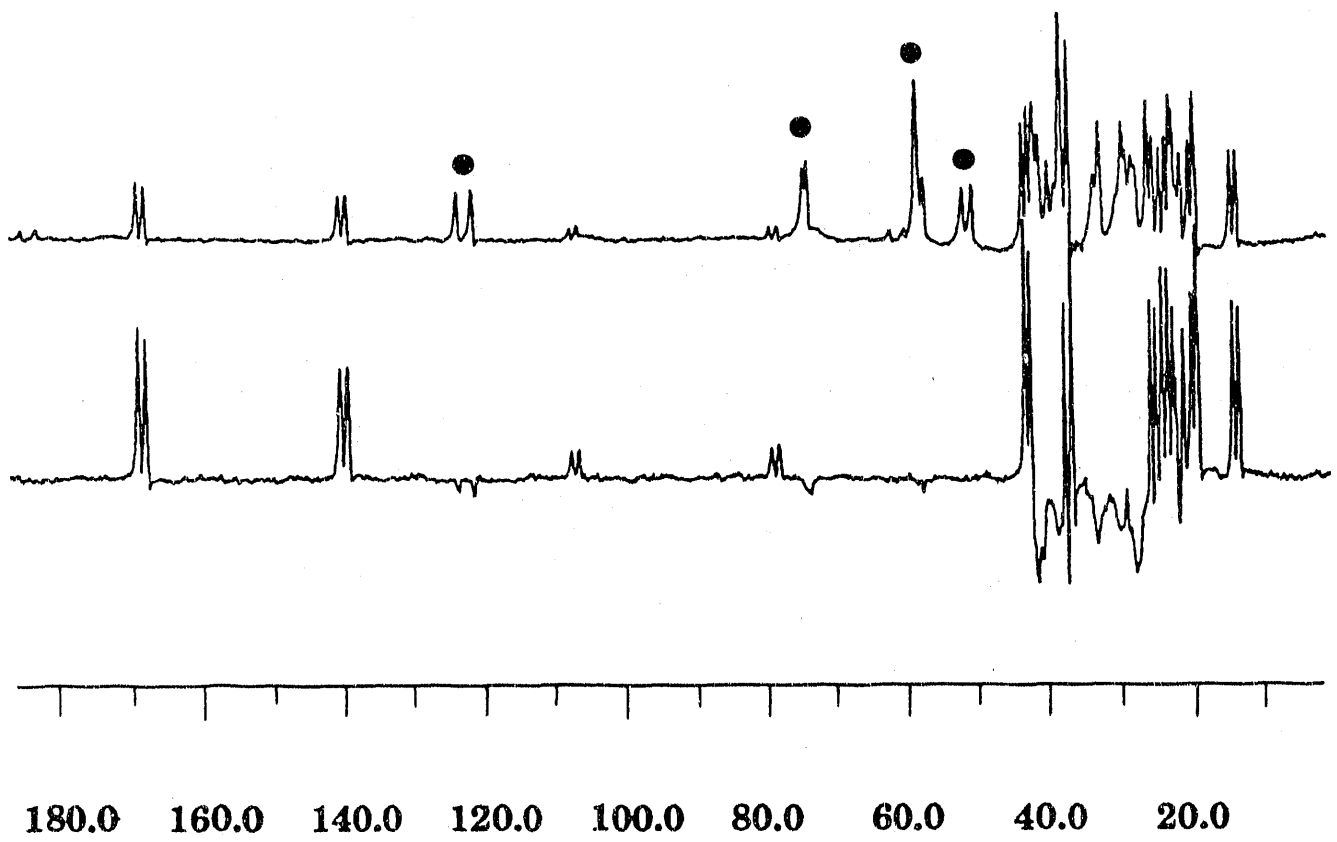

Figure 8

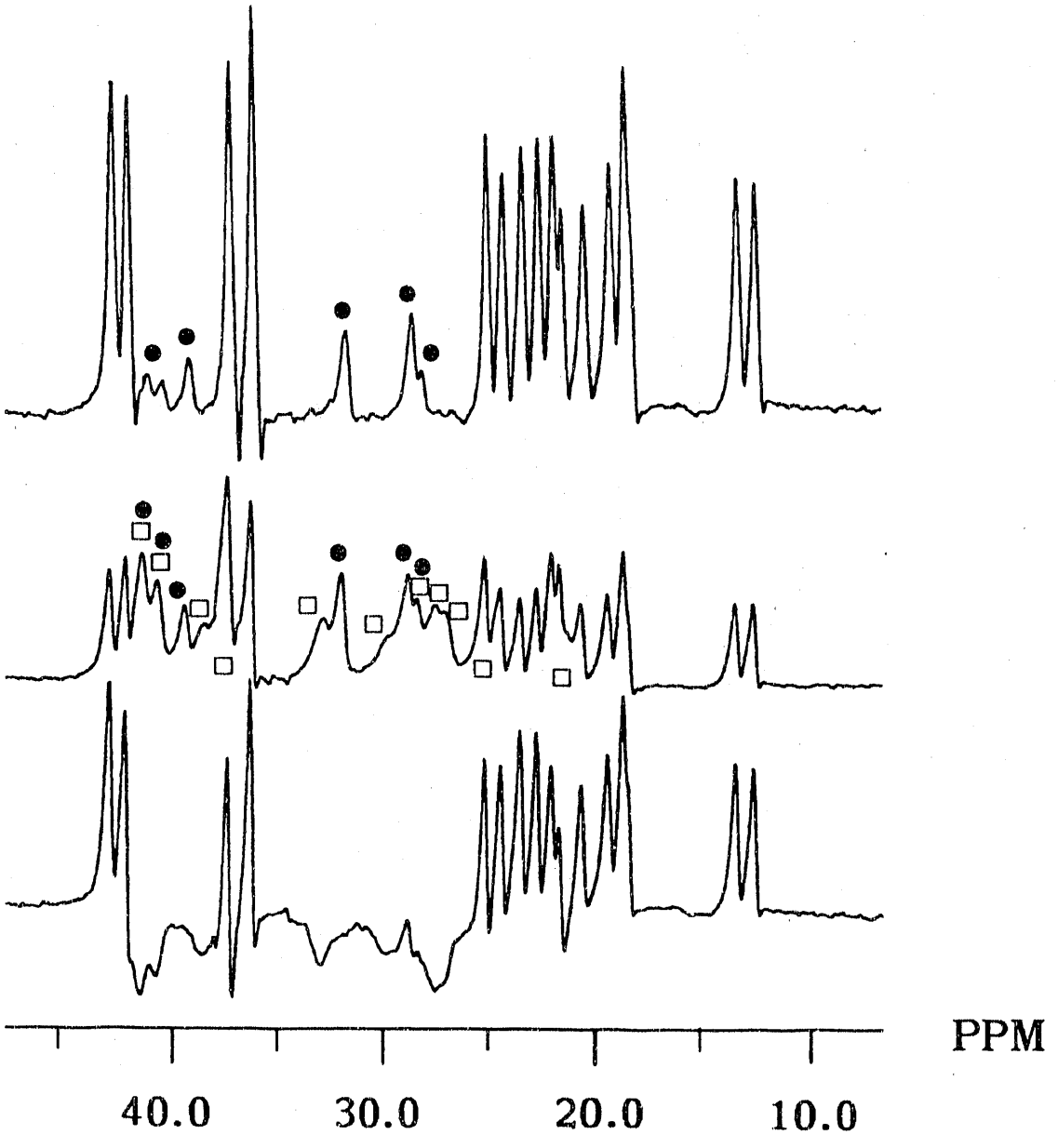

Figure 9

END

DATE
FILMED
11/5/92